MRS Communications (2019), *9*, 344–351
© Materials Research Society, 2019
doi:10.1557/mrc.2018.238

MRS Communications

Research Letter

Biocompatible methionine-capped CdS/ZnS quantum dots for live cell nucleus imaging

S. Kanagasubbulakshmi, I. Gowtham, and **K. Kadirvelu,** DRDO—BU Center for Life Sciences, Bharathiar University Campus, Coimbatore, 641046, India
K. Archana, Department of Biotechnology, PSG College of Arts & Science, Coimbatore, 641014, India
Address all correspondence to K. Kadirvelu at **kadirvelukrishna@yahoo.com**

(Received 22 August 2018; accepted 17 December 2018)

Abstract

CdS/ZnS core shell quantum dots (QDs) were synthesized and functionalized by methionine and characterized by standard techniques. The prior QD-based phytotoxicity assay was helpful to find out the maximum tolerant level of the plant cells. The successful transport and phytotoxic mechanism of QDs were elaborated in detail. Methionine functionalities on the QDs were helpful in specific binding of QDs with the nucleus of stomata in plant cells. Target specific interaction with the nucleus of stomata cells was a novel breakthrough that can be used in many biologic applications.

Introduction

The quantum dots (QDs) have received significant attention in current research scenario in terms of stable photophysical properties. QDs have been known for their unique emission spectra which can be tuned to obtain entire visible to near-infrared spectra.[1–5] The bioimaging and biolabeling of animal and plant cells require excellent photostability of the fluorescent compound when compared to organic dyes and other fluorescent tags.[6] Current technologies to address the photostability depend on nanoengineering of the materials. However, there are various emerging fields which have been using engineered materials starting from day to day applications to defense technologies. The research findings in designing of nanomaterials differ in each application that supplement target-based functionalities on the surface of the nanomaterial.

In particular, the biologic applications of QDs have unique sets of challenges in terms of designing of target-based functional groups and biocompatibility. The semiconductor-based QDs are known for their toxic effects in an environment that need rigorous analysis to address the harmful effects. Although the reports about cytotoxicity of QDs on human cells are available enormously, the findings of environment tolerance level still require additional assessment using plant system. To date, there are very limited reports only available about the sole understanding of QD toxicity to plant system.[7]

Plants have a vital role in the environment as they directly come in contact with the contaminants that have been accumulated in the soil.[8] Once the QDs have exposed to the plant system they have been transported through aerial or the root pathway. The bioaccumulation of QDs can have either beneficial or adverse effect on the plant system. The QDs at higher concentration suppress the plant growth and enhances it at lowest concentrations.[9] The developed technologies in nanoscience laid a platform to use QDs as a biomarker in plant science. The recent studies have reported that the fluorescent QDs can be used as a phenomenal alternative substrate to conventional materials.[10–12]

The applications of QDs have drawn a significant attention in plant science as it can be used as a marker to distinguish the organelles in plant cell. This fact was proven by CdSe QDs attachment toward the cell wall of *Picea omorika*.[13] The physiochemical characteristics of QDs lead to the polymeric interaction with the cell wall of plant cells and enabled the QDs as a significant labeling agent. The previous studies about QD interaction with the plant system have reported the analysis of the toxic profile through the penetration of QDs in plants.[9,14] Among other QDs, the CdS-based semiconductors have unique photophysical properties with a band gap (2.42 eV) that has paved the platform to many applications.[15] The core shell CdS/ZnS QDs are well surface passivated that enables high fluorescent stability inside the biologic system without blinking.[16] Methionine residues are proven endogenous antioxidants[17] effectively used as a stabilizing agent in AuNps[18] and magnetic NPs[19] production.

In this study, CdS/ZnS core shell QDs were synthesized and functionalized by methionine that helps to interact with biomolecules. Amino acid-based functional groups on the QD surface paved a way to design a plant cell-based study. *Vigna radiata* was used as a model plant for the phytotoxicity assessment since it is recognized as a test species for terrestrial phytotoxicity by OCED (Organization for economic co-operation and development). *V. radiata* was chosen as a model plant as it is

https://doi.org/10.1557/mrc.2018.238 Published online by Cambridge University Press

one of the fast-growing plants that can support to analyze the effects of QDs in the plant system within the study period. *Nicotiana benthamiana* plant model was used to achieve the biolabeling since it has less chlorophyll content that could avoid background interferences. *V. radiata* and *N. benthamina* were chosen as ideal plants to investigate the cytotoxicity profile and imaging potential of methionine-functionalized CdS/ZnS QDs.

Experimental section

Analar grade (AR) cadmium chloride ($CdCl_2{\cdot}5H_2O$), sodium sulfide (Na_2S), trisodium citrate, zinc chloride ($ZnCl_2$), and methionine were obtained from Sigma Aldrich.

Synthesis of CdS/ZnS core shell QDs

Hydrophilic CdS/ZnS QDs were synthesized by well-established methodology[5] with minor modifications. Briefly, water-soluble methionine-functionalized CdS QDs were synthesized by the reflux condensation method. In that, the primary monomers ratio of CdS core was maintained as 1:2 ($CdCl_2{\cdot}5H_2O$:Na_2S) and trisodium citrate were used as a reducing agent. The CdS core formation was maintained in 150 mL of double distilled water at 120 °C for 1 h. The ZnS shell on the CdS core QDs was passivated using equimolar solution of $ZnCl_2$ and Na_2S. Surface capping was done using methionine by stirring the core shell QDs along with amino acid at room temperature. The precipitated methionine-capped CdS/ZnS QDs were dried under vacuum conditions at 60° C for 30 min and used further for characterizations and applications.

Phytotoxicity assessment

The stock solutions of QDs were prepared at concentrations of 25, 50, 100, 200, 300, 400, and 500 µg/mL. The seeds of *V. radiata* were imbibed to sprout in sterile Petri plates, on two layers of Whatman filter-paper drenched with various concentrations of prepared QDs.[20] The plates were maintained for 3 days under optimal growth conditions (in vitro). Seed germination percentage, phytotoxicity were calculated by the formulae given by Meena et al. and the vigor index and tolerance indices were calculated using following formulae:

$$\text{The vigor index} = (\text{Mean root length} + \text{Mean hypocotyls/Shoot length}) \times \%\ \text{Germination}$$

$$\text{Tolerance indices} = \frac{\text{Mean root length in metal solution}}{\text{Mean root length in distilled water}} \times 100$$

$$\text{Phytotoxicity} = \frac{\text{Control shoot or root length} - \text{Treated shoot or root length}}{\text{Control shoot or root length}} \times 100$$

DPPH radical scavenging activity

The 2,2-diphenyl-1-picrylhydrazyl (DPPH) assay was done by following the existing methodology[21] with minor modifications. The 0.1 mM of DPPH was dissolved in methanol, 25 µL of QD-treated plant extract and 475 µL of Tris HCl was added. The reaction mixture was mixed well and maintained in the absence of light at 28 °C for 30 min. The blank contains 25 µL of methanol, 475 µL of Tris HCl, and 1 mL of DPPH and the blank was maintained without DPPH and the absorbance spectra were taken at 517 nm. The percentage radical scavenging activity of QDs was determined by below formula:

$$\%\ \text{of radical scavenging activity} = \frac{1 - \text{Absorbance of sample}}{\text{Absorbance of control}} \times 100$$

Characterization techniques

The photophysical properties of QDs were confirmed by standard laboratory methods. UV-visible spectrum was obtained by a UV-Vis-NIR spectrophotometer (Shimadzu 3600 model) and emission spectra by a spectrofluorometer (Horiba JobinYvonFluromax 4). Zeta potential was determined by a Zetasizer Malvern and the uniform size distribution and crystallinity were analyzed by HR-TEM (JOEL JEM 2100 at 200 kV). FT-IR spectra were obtained by FT-IR (Shimadzu 8400S model). Fluorescence imaging was obtained using an inverted fluorescence microscope (long-pass filters) (EVOS).

Bioimaging

The dosage of QDs (25 µg/mL) for plant cell imaging was fixed by phytotoxicity assay. As fixed dosage of QDs was used to image the shoot cross-section of *Nicotiana benthamiana* and peeled out an epidermal layer of *V. radiata.* The images were captured using Olympus CKX41 JENOPTIK Fluorescence microscope.

Results and discussion

This study was mainly focused on obtaining hydrophilic QDs with target-specific functional groups (NH_2 and COOH) by an aqueous synthesis method. Since the study is about the interaction of QDs with plant system the toxicity was considered as a major factor to be reduced. The leaching and surface oxidation of cadmium (Cd) ions leads to the potential toxic effects in a living system. The proper surface passivation of QDs enhances the photophysical properties, provide monodispersed platform and reduces the cytotoxicity of QDs.[22] The higher bandgap shell (ZnS) coverage prevents the oxidation as well as leaching of Cd ions into the surrounding matrix. Methionine functional groups were found to be target specific without affecting the quantum efficiency of QDs.

The core shell QD interaction with guard cells of a plant leaf is graphically illustrated in Fig. 1. The UV-visible spectra of CdS and CdS/ZnS QDs are shown in Fig. S1(a). The ZnS passivation on the CdS QDs has increased absorbance wavelength

https://doi.org/10.1557/mrc.2018.238 Published online by Cambridge University Press

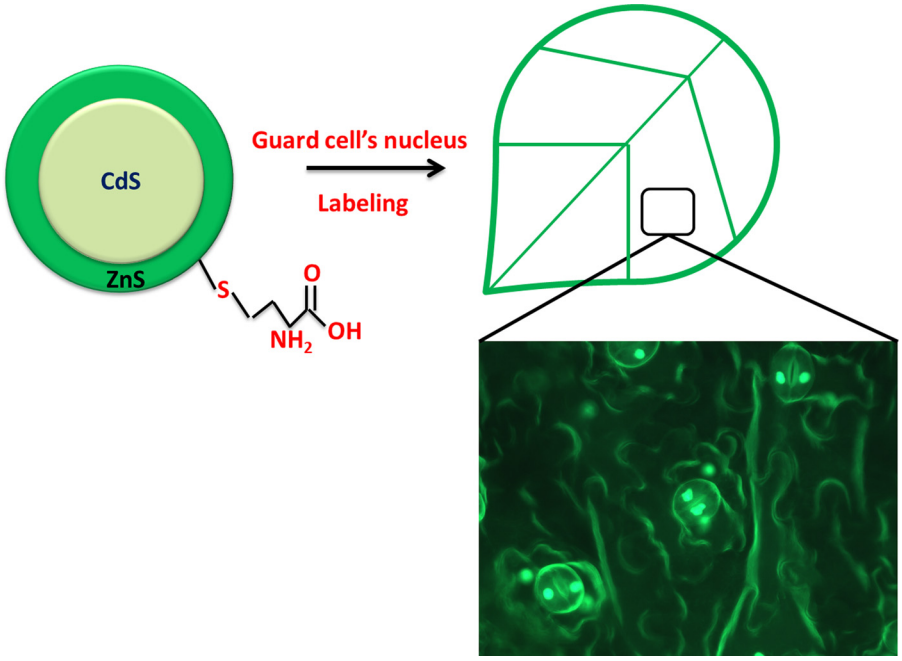


Figure 1. Schematic outline of the steps involved in nucleus labeling.

from 440 to 450 nm and decreased the bandgap from 2.8 to 2.7 eV. The band gap was calculated using $E = hc/\lambda$, where E = energy, h = Planck's constant, ν = frequency of light, c = speed of light, and λ = wavelength of light. The photoluminescence (PL) spectra are depicted in Fig. 2(b) that denoted the fluorescence color emission of QDs. The high monodispersity of the QDs was confirmed since there was no other peaks in the PL spectrum.[23]

The prominent surface passivation and regulation in electron mobility leads to phenomenal increase in PL spectra as shown in Fig. 1(b).[24,25] The PL intensity enhancement was observed in core shell QDs due to the higher bandgap material (ZnS) passivation. The surface passivation by the shell reduces the defect sites and gives the controlled emission of QDs and enhancing the PL intensity. The elemental compositions [Figs. S1(c) and S1(d)] of CdS and CdS/ZnS QDs were analyzed to confirm the presence of ZnS shell on the CdS QDs.

The typical HR-TEM micrograph of size distribution and morphology of the water-soluble methionine-capped CdS/ZnS QDs are shown in Figs. 2(a) and 2(b). The core shell formation was confirmed by the dark core and lighter shell around it. The average size and interplanar spacing [Fig. 2(c)] of the QDs are calculated as 6.5 and 0.2051 nm, respectively (ImageJ software). The uniform and non-aggregated distribution of QDs was maintained by methionine capping. The selected area electron diffraction (SAED) pattern of QDs is shown in Fig. 2(d). The well-resolved lattice fringes prove the crystalline property of the QDs and crystal planes (311), (220), and (111) derived from the pattern were consistent with the JCPDS card no #75-0581 that confirms the cubic zinc blende structure of QDs. The hydrodynamic radii of the core (3.2 nm), core shell—CdS/ZnS QDs (6.4 nm), and methionine-capped CdS/ZnS QDs (8.3 nm) were analyzed to monitor the change in size distribution of QDs (Figs. S2–S4). From zeta potential measurement, the surface charges of CdS and CdS/ZnS core shell QDs were found to be −26 and −29.2 mV respectively. Amino acid capping has enhanced the surface negative charge (−44.2 mV) of QDs by target specific functional groups (Figs. S5–S7).

FT-IR spectra were recorded for methionine-capped CdS/ZnS core shell QDs (Fig. S8). The stretching at C–S 1430/cm confirms the methionine interaction with QDs.[5,26] The symmetric vibration of C═O (1629 and 1690/cm), and S–H stretch (951.84/cm), C–N (1013, 1194/cm), and C–S (739/cm) were attributed to methionine functional groups on the QD surface. Methionine was attached on the QDs through C–S bonding and leaves –COOH and $–NH_2$ groups for further interaction.[5]

QD interaction with the plant system

Generally, the toxicity of QDs must have to be analyzed as it has been closely interacting with the environment through various applications. However, the unique optical properties helped to achieve a quality imaging in plant system.[27,28] Here, *V. radiata* was used as testing plant to analyze the phytotoxicity.

The growth of root and stem were differed from the control groups in treatment condition as depicted in Fig. S9. Higher concentration of QDs has affected the growth of *V. radiata* and the average seedling length of the plant decreased from 16.5 to 2.5 cm on the other hand average shoot length of the

https://doi.org/10.1557/mrc.2018.238 Published online by Cambridge University Press

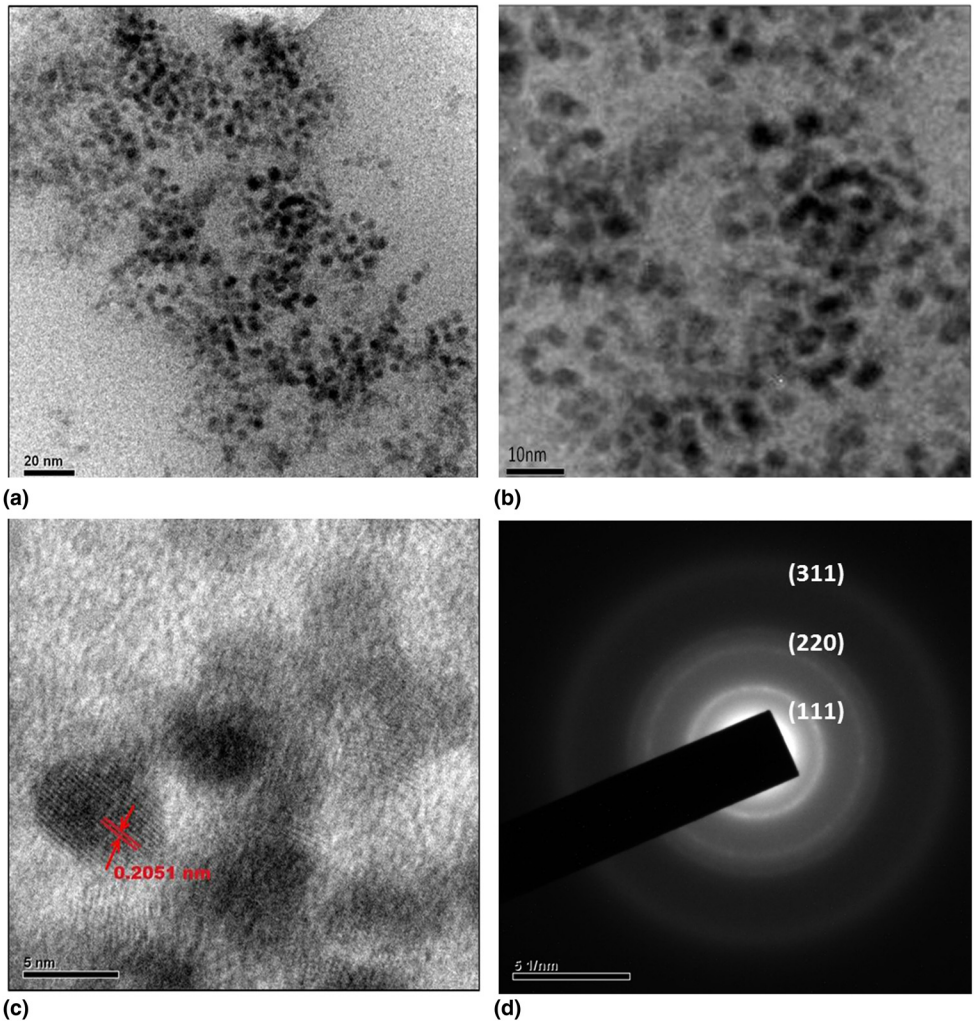


Figure 2. (a) and (b) HR-TEM images of methionine-capped CdS/ ZnS QDs at 10 and 20 nm scale magnification. (c) Interplanar spacing of QDs–0.2051 nm. (d) SAED pattern of methionine-capped CdS/ZnS QDs.

plant has decreased from 7.5 to 2.2 cm. The average root length of *V. radiata* decreased from 9.3 to 1.1 cm. Seedling vigor index was high at less concentration of QDs (25 μg/mL) and found to be less at higher concentration (500 μg/mL). The average seedling vigor index of *V. radiata* was decreased from 2% to 90% and the tolerance index decreased from 17% to 90% with the proportion to QD concentration. The experiments were found to be statistically significant ($P < 0.005$) that was analyzed by one way analysis of variance (Fig. S10).

At higher concentration, the metal ions leaching from metallic QDs cause the significant stress in the growth of the plants. However, the seed coat permeability remains constant and shoot and root elongation was observed in all concentration of QDs. The significant reduction of growth at a higher concentration of QDs can be correlated with oxidative stress induced radicals that causes a dose-dependent response.[20] The heavy metal transport-based mechanism in plants can be evoked as an explanation for the phytotoxicity of QDs. Generally, the Cd^{2+} ions leaching from the QDs cause the dose-dependent toxicity and suppress the seed germination in very low-level concentration. To overcome the leaching of Cd^{2+} ions from the core QDs, the surface passivation by ZnS has been followed and amino acid capping also helped in arresting of Cd^{2+} ions at the maximum.[29,30] Elevated levels of DPPH activity [Fig. S10 (d)] denote the plant counter defense against the QDs exposure to the seedlings.

While increasing the concentration of QDs from 25 to 500 μg/mL the proportional decrease in the plant growth was observed. Moreover, an uncharacteristic increase of phytotoxicity, vigor index, and low DPPH activity was also observed among the treatment groups. The non-monotonic dose–responses were due to the paradoxical effects and hormesis of the heavy metal (CdS/ZnS)-derived QDs explored in this study. Similarly, the study involves the mathematical model

https://doi.org/10.1557/mrc.2018.238 Published online by Cambridge University Press

development for the heavy metal (Zn/Cd/Ni/Pb) impact on sunflower seedlings has shown non-monotonic dose–responses in germination percentage, shoot/root length.[31] The study involves the quantification of paradoxical and hormesis effects of wheat seedlings exposed to various pollutants estimated 85.7% (of which hormesis was 5.5% and paradoxical effects were 94.5%) of dose responsive dependencies were non-monotonic.[32] In all denotable parameters [phytotoxicity, vigor index, tolerance index, radical scavenging activity—Figs. S10(a)–S11(d)], the effect of QDs was significantly varied beyond 100 μg/mL concentration; this was due to the activity of P-type heavy metal ATPase activity in plants.[33] The P-type heavy metal ATPase was found in many plants mainly helps in the passage of heavy metals through the cell membrane. When the QD concentration increases beyond such limit (100 μg/mL) it decreases the enzyme activity significantly and non-uniform effects were observed in all parameters.

The positive and negative effects of the elements mainly depend on the concentration and its chemical nature of binding. Generally, the positive effects were observed when the essential elements were present in very low concentration. The higher concentration of heavy metal ions (Cd^{2+}) leads to the inhibition of cytoplasmic enzymes and damage to the cell membrane. On the other hand, the Cd^{2+} ions indirectly affect the plant growth by replacing the essential elements in cation binding sites of plants.[34] The same mechanism can be taken as the explanation for the suppressed growth of the plants when we increase the QD concentration.

Visualization of QDs in a plant system

The QDs have high potential when compared to traditional organic dyes and can be used in immunolabeling applications.[35] The successful demonstration of QDs with the interaction with plant's reproductive parts have proven its efficiency in plant cell imaging.[36] Herein we report that target specific QDs could bind with plant cells and visualize the targeted domain. In a previous study,[37] the QDs uptake and the fluorescence were not able to be distinguished because of the plant's autofluorescence. To overcome those issues, *N. benthamina* was chosen for imaging purpose since the chlorophyll interferences were less when to compare to higher plants to monitor the interaction of QDs with plant cell. Consistent with the literature, *N. benthamina* was able to uptake QDs through membrane transporters which further assist QDs entry through the hydrophobic lipid bilayer. The QDs uptake through shoot is shown in Fig. 3, which clearly proves its fluorescent capability by staining the xylem part of the plant cell. The minimum dose concentration that influences the plant growth was calculated from phytotoxicity studies and further used in plant cell imaging. Since the QDs are hydrophilic which could transport via the xylem region, the plant shoot cross-section was used to provide specific insights about translocation of QDs in a plant system.

The tracheary elements like xylem cells help in the transportation of essential water and minerals.[38] Tracheary elements transport the QDs and uniformly bind with the cell wall, Fig. 3 shows that fluorescence of QDs was stable inside the cell and autofluorescence was compared with treated cells. This factor was found to be phenomenal in the application of plant cell imaging.

So far the studies[7,36] those report only the agglomeration of QDs on the plant cell tissues through uptake from the medium. The nucleus-specific binding of DAPI (4′,6-diamidino-2-phenylindole) dye for nuclear localization[39] was also found to be less significant due to its photobleaching effect and less quantum efficiency when compared to semiconductor QDs. Our finding of specific insight into the QD interaction with plant cell at the nucleus level (Fig. 4) would be a novel concept in live cell imaging.

Mechanism of nucleus labeling by QDs

Normal plant cell functions can elucidate the mechanism of QDs uptake into the nucleus as described below. Generally, the uptake of potassium ions into guard cell causes the stomatal opening and potassium ion pumps have the main role in the opening of stomatal apertures. The subsequent release of negatively charged ions into the intracellular surface of the guard cell plasma membrane leads to a positive voltage shift. Thus,

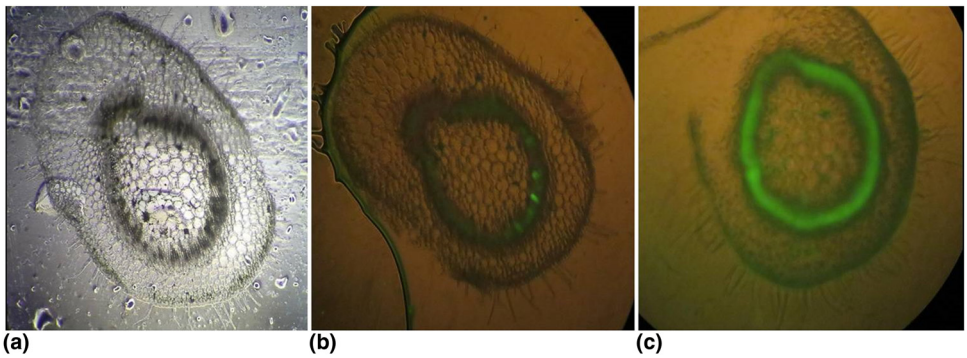


Figure 3. *N. benthamina* live cells images (a) under bright field (cross-section of the shoot), (b) control, and (c) uptake QDs in the xylem region and its green fluorescence.

https://doi.org/10.1557/mrc.2018.238 Published online by Cambridge University Press

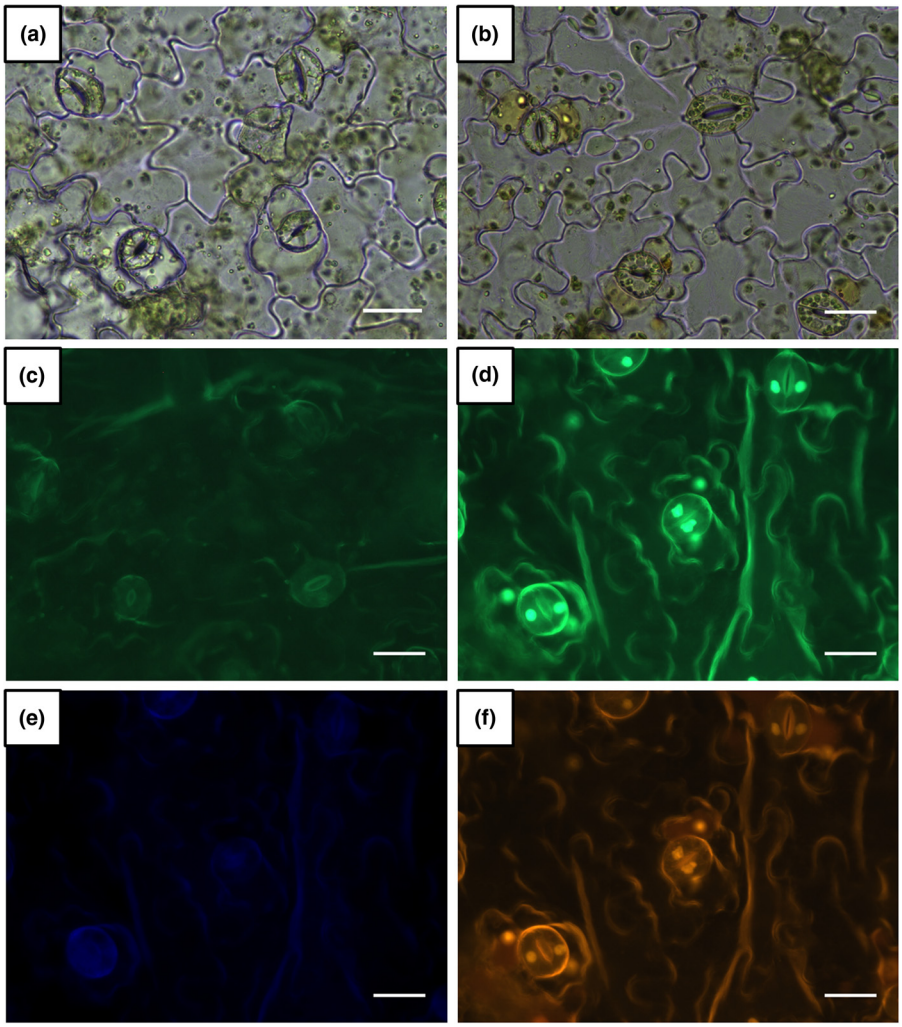


Figure 4. A lower epidermal layer of *N. benthamina* live cell imaging: (a) control leaf section, (b) leaf section stained with (25 µg/mL) QDs visualized under white light, (c) unstained control, (d–f) QDs stained (25 µg/mL) section visualized under UV with GFP, DAPI, and red fluorescence filter.

the positively charged surface of cell membrane effectively binds with negatively charged QDs and allows successful penetration inside the guard cells which facilitates QDs to bind with the nucleus. Methionine was used as an effective stabilizing agent and proven capping agent to prepare biocompatible nanoparticles. N-terminal methionine residues in the transcription factors are the major determinant facilitates the interaction with the DNA.[40] This successful target-based delivery of QDs into the nucleus can be used in the stomatal index-based studies efficiently.

The toxic effect of QDs in the guard cells was found to be less significant as it has not altered the morphology or signaling of the system. For in vitro applications, the QDs uptake and target specific interaction with cells is essential to interpret the mechanism of binding. In previous studies,[41–44] the QDs have been used as the biolabeling agent for proteins, lipopolysaccharide and lectin to investigate the specificity and anticancer activity. According to our knowledge, this is a first report which has focused on methionine-capped CdS/ZnS QDs in target specific imaging of nucleus in plant cells. Our studies have proven that the phytotoxicity of QDs is very less due to the efficient surface coating that prevents surface oxidation and leaching of cadmium ions into the plant system. The live plant cell imaging can be improved with the proper elucidation of QD penetration to the plant cells by live tracking methodology.

Conclusion

The water-soluble methionine-capped CdS/ZnS QDs were synthesized and characterized to define its photophysical properties. The effective surface passivation covers the lattice mismatches and provides enhanced PL intensity. Target-based functionalization helped to study the interactions between QDs and plant. The phytotoxic effect on plant growth was found in the

https://doi.org/10.1557/mrc.2018.238 Published online by Cambridge University Press

concentration range of QDs from 25 to 300 μg/mL. The uptake of QDs in *N. benthamina* and distribution of QDs in cross-section of the shoot was visualized under fluorescence microscopy. The specific binding and penetration of QDs into the nucleus of guard cells (*N. benthamina*) was a novel approach that can help in many stomatal index-based studies.

Supplementary material

The supplementary material for this article can be found at https://doi.org/10.1557/mrc.2018.238.

Acknowledgment

The authors (S. Kanagasubbulakshmi and I. Gowtham) would like to thank DRDO for providing fellowship. This work was financially supported by DRDO.

References

1. H. Mattoussi, J. Matthew Mauro, E.R. Goldman, G.P. Anderson, V. C. Sundar, F.V. Mikulec, and M.G. Bawendi: Self-assembly of CdS-ZnS quantum dot bioconjugates using an engineered recombinant protein. *J. Am. Chem. Soc.* **122**, 12142–12150 (2000).
2. Z.A. Peng and X. Peng: Formation of high-quality CdTe, CdSe, and CdS nanocrystals using CdO as precursor. *J. Am. Chem. Soc.* **123**, 183–184 (2001).
3. B.O. Dabbousi, J. Rodriguez-Viejo, F.V. Mikulec, J.R. Heine, H. Mattoussi, R. Ober, K.F. Jensen, and M.G. Bawendi: (CdSe) ZnS core–shell quantum dots: synthesis and characterization of a size series of highly luminescent nanocrystallites. *J. Phys. Chem. B.* **101**, 9463–9475 (1997).
4. W.C.W. Chan and S. Nie: Quantum dot bioconjugates for ultrasensitive nonisotopic detection quantum dot bioconjugates for ultrasensitive non-isotopic detection. *Science* **281**, 2016–2018 (1998).
5. M. Bruchez, M. Moronne, P. Gin, S. Weiss, and A. Paul Alivisatos: Semiconductor nanocrystals as fluorescent biological labels. *Science* **5385**, 2013–2016 (1998).
6. X. Michalet, F.F. Pinaud, L.A. Bentolila, J.M. Tsay, S.J.J.L. Doose, J.J. Li, G. Sundaresan, A.M. Wu, S.S. Gambhir, and S. Weiss: Quantum dots for live cells, in vivo imaging, and diagnostics. *Science* **5709**, 538–544 (2005).
7. M. Alimohammadi, Y. Xu, D. Wang, A.S. Biris, and M.V. Khodakovskaya: Physiological responses induced in tomato plants by a two-component nanostructural system composed of carbon nanotubes conjugated with quantum dots and its in vivo multimodal detection. *Nanotechnology.* **29**, 295101 (2011).
8. D.S. Lidke, K.A. Lidke, B. Rieger, T.M. Jovin, and D.J. Arndt-Jovin: Reaching out for signals: filopodia sense EGF and respond by directed retrograde transport of activated receptors. *J. Cell Biol.* **4**, 619–626 (2005).
9. W. Li, Y. Zheng, H. Zhang, Z. Liu, W. Su, S. Chen, Y. Liu, J. Zhuang, and B. Lei: Phytotoxicity, uptake, and translocation of fluorescent carbon dots in mung bean plants. *ACS Appl. Mater. Interfaces* **8**, 19939–19945 (2016).
10. R.C. Monica and R. Cremonini: Nanoparticles and higher plants. *Caryologia* **62**, 161–165 (2009).
11. R. Nair, A.C. Poulose, Y. Nagaoka, Y. Yoshida, T. Maekawa, and D. Sakthi Kumar: Uptake of FITC labeled silica nanoparticles and quantum dots by rice seedlings: effects on seed germination and their potential as biolabels for plants. *J. Fluoresc.* **21**, 2057–2068 (2011).
12. J. Peng, Y. Sun, Q. Liu, Y. Yang, J. Zhou, W. Feng, X. Zhang, and F. Li: Upconversion nanoparticles dramatically promote plant growth without toxicity. *Nano Res.* **5**, 770–782 (2012).
13. Y. Koo, J. Wang, Q. Zhang, H. Zhu, E. Wassim Chehab, V.L. Colvin, P.J. J. Alvarez, and J. Braam: Fluorescence reports intact quantum dot uptake into roots and translocation to leaves of Arabidopsis thaliana and subsequent ingestion by insect herbivores. *Environ. Sci. Technol.* **49**, 626–632 (2015).
14. D. Chakravarty, M.B. Erande, and D.J. Late: Graphene quantum dots as enhanced plant growth regulators: effects on coriander and garlic plants. *J. Sci. Food Agric.* **95**, 2772–2778 (2015).
15. M. Thambidurai, N. Muthukumarasamy, S. Agilan, N. Sabari Arul, N. Murugan, and R. Balasundaraprabhu: Structural and optical characterization of Ni-doped CdS quantum dots. *J. Mater. Sci.* **46**, 3200–3206 (2011).
16. F. Mirnajafizadeh, F. Wang, P. Reece, and J. Arron Stride: Synthesis of type-II CdSe (S)/Fe_2O_3 core/shell quantum dots: the effect of shell on the properties of core/shell quantum dots. *J. Mater. Sci.* **51**, 5252–5258 (2016).
17. R.L. Levine, L. Mosoni, B.S. Berlett, and E.R. Stadtman: Methionine residues as endogenous antioxidants in proteins. *Proc. Natl. Acad. Sci.* **93**, 15036–15040 (1996).
18. A. Javed Raza, S.M.Z. Qureshi, and M.S. Khan: Synthesis and study of catalytic application of l-methionine protected gold nanoparticles. *Appl. Nanosci.* **7**, 429–437 (2017).
19. A. Jagminas, A. Mikalauskaite˙, V Karabanovas, and J. Vaičiu¯niene˙: Methionine-mediated synthesis of magnetic nanoparticles and functionalization with gold quantum dots for theranostic applications. *Beilstein J. Nanotechnol.* **8**, 1734 (2017).
20. T. Pazhanivel, D. Nataraj, V.P. Devarajan, V. Mageshwari, K. Senthil, and D. Soundararajan: Improved sensing performance from methionine capped CdTe and CdTe/ZnS quantum dots for the detection of trace amounts of explosive chemicals in liquid media. *Anal. Methods* **5**, 910–916 (2013).
21. D. Lin and B. Xing: Phytotoxicity of nanoparticles: inhibition of seed germination and root growth. *Environ. Pollut.* **150**, 243–250 (2007).
22. M.S. Blois: Antioxidant determinations by the use of a stable free radical. *Nature* **181**, 1199–1200 (1958).
23. C. Zhai, H. Zhang, N. Du, B. Chen, H. Huang, Y. Wu, and D. Yang: One-pot synthesis of biocompatible CdSe/CdS quantum dots and their applications as fluorescent biological labels. *Nanoscale Res. Lett.* **6**, 1–5 (2011).
24. M. Li, H. Zhou, H. Zhang, P. Sun, K. Yi, M. Wang, Z. Dong, and S. Xu: Preparation and purification of L-cysteine capped CdTe quantum dots and its self-recovery of degenerate fluorescence. *J. Lumin.* **130**, 1935–1940 (2010).
25. G. Gaur, D.S. Koktysh, D.M. Fleetwood, R.A. Weller, R.A. Reed, B. R. Rogers, and S.M. Weiss: Influence of ionizing radiation and the role of thiol ligands on the reversible photodarkening of CdTe/CdS quantum dots. *ACS Appl. Mater. Interfaces* **8**, 7869–7876 (2016).
26. P. Thangadurai, S. Balaji, and P.T. Manoharan: Surface modification of CdS quantum dots using thiols—structural and photophysical studies. *Nanotechnol.* **19**, 435708 (2008).
27. F. Mohammad and H.A. Al-Lohedan: Toxicity assessment of engineered Mn–ZnS quantum dots in vitro. *J. Mater. Sci.* **51**, 9207–9216 (2016).
28. Q. Liu, Y. Zhao, Y. Wan, J. Zheng, X. Zhang, C. Wang, X. Fang, and J. Lin: Study of the inhibitory effect of water-soluble fullerenes on plant growth at the cellular level. *ACS Nano* **4**, 5743–5748 (2010).
29. A. Hoshino, K. Fujioka, T. Oku, and M. Suga: Physicochemical properties and cellular toxicity of nanocrystal quantum dots depend on their surface modification. *Nano Lett.* **4**, 2163–2169 (2004).
30. R. Xing, X.D. Chen, Y.F. Zhou, J. Zhang, Y.Y. Su, J.F. Qiu, Y.H. Sima, K. Q. Zhang, Y. He, and S.Q. Xu: Targeting and Retention Enhancement of Quantum Dots Decorated with Amino Acids in an Invertebrate Model Organism. *Sci. Rep.* **6**, 1–10 (2016).
31. X. Zhao, J. Joo, D. Kim, J. Lee, and J.Y. Kim: Estimation of the Seedling Vigor Index of Sunflowers Treated with Various Heavy Metals. *J. Biorem. Biodegrad.* **7**, 1–6 (2016).
32. E.A. Erofeeva: Hormesis and paradoxical effects of wheat seedling (*Triticum aestivum* L.) parameters upon exposure to different pollutants in a wide range of doses. *Dose. Response.* **12**, 121–135 (2014).
33. I. Yruela: Copper in plants. *Brazilian J. Plant Physiol.* **1**, 145–156 (2005).
34. G.U. Chibuike and S.C. Obiora: Heavy metal polluted soils: effect on plants and bioremediation methods. *Biorem. Meth.* **2014**, 1–12 (2014).

https://doi.org/10.1557/mrc.2018.238 Published online by Cambridge University Press

35. F. Müller, A. Houben, P.E. Barker, Y. Xiao, J.A. Käs, and M. Melzer: Quantum dots—a versatile tool in plant science? *J. Nanobiotechnol.* **4**, 5 (2006).
36. S. Ravindran, S. Kim, R. Martin, E.M. Lord, and C.S. Ozkan: Quantum dots as bio-labels for the localization of a small plant adhesion protein. *Nanotechnology* **16**, 1–4 (2005).
37. N. Al-Salim, E. Barraclough, and E. Burgess: Brent Clothier, Markus Deurer, Steve Green, Louise Malone, and Graham Weir: Quantum dot transport in soil, plants, and insects. *Sci. Total Environ.* **409**, 3237–3248 (2011).
38. K.A. McCulloh, J.S. Sperry, and F.R. Adler: Water transport in plants obeys Murray's law. *Nature* **6926**, 939 (2003).
39. M. Libault, F. Tessadori, S. Germann, B. Snijder, P. Fransz, and V. Gaudin: The Arabidopsis LHP1 protein is a component of euchromatin. *Planta* **222**, 910–925 (2005).
40. D. Meierhans and R.K. Allemann: The N-terminal methionine is a major determinant of the DNA binding specificity of MEF-2C. *J. Biol. Chem.* **273**, 26052–26060 (1998).
41. L.S. Mgcina, I.A. Dubery, and L.A. Piater: Comparative conventional-and quantum dot-labeling strategies for LPS binding site detection in Arabidopsis thaliana mesophyll protoplasts. *Front. Plant Sci.* **6**, 1–11 (2015).
42. D. Djikanović, A. Kalauzi, M. Jeremić, J. Xu, M. Mićić, J.D. Whyte, R. M. Leblanc, and K. Radotić: Interaction of the CdSe quantum dots with plant cell walls. *Colloids Surf., B* **91**, 41–47 (2012).
43. K.B.A. Ahmed, P. Ahalya, M. Sengan, R. Kamlekar, and VeerappanA.: Synthesis and characterization of zinc sulfide quantum dots and their interaction with snake gourd (*Trichosanthes anguina*) seed lectin. *Spectrochim. Acta—Part A: Mol. Biomol. Spectrosc.* **151**, 739–745 (2015).
44. D.A. Navarro, M.A. Bisson, and D.S. Aga: Investigating uptake of water-dispersible CdSe/ZnS quantum dot nanoparticles by Arabidopsis thaliana plants. *J. Hazard. Mater.*, **211–212**, 427–435 (2012).

https://doi.org/10.1557/mrc.2018.238 Published online by Cambridge University Press